CHAPTER 31

EVALUATION OF NUMERICAL MODELS ON WAVE-CURRENT INTERACTIONS

Jung L. Lee[1] and Hsiang Wang [2]

Abstract

Five comtemporary numerical models on wave-current interactions are evaluated in this paper. The bases of evaluation are mathematical exactness, degree of computational difficulty and practical applicability in terms of the abilities of handling shoaling, refraction, diffraction, reflection and wave-current interaction. Recommendations are given in matrix form on the relative merit of each model.

1 Introduction

In the past two decades, we have witnessed remarkable progress in modeling nearshore hydrodynamics by numerical techniques. Prediction of nearshore waves took a new dimension with the introduction of the mild slope equation by Berkhoff (1972) which is capable of handling the combined effects of refraction and diffraction. Since then significant progress has been made in computational techniques as well as model capabilities, notably by Radder (1979), Copeland (1985), Ebersole (1986), Yoo and O'Connor (1986a), and Dalrymple et al. (1989).

Prediction of nearshore, wave-induced currents has also advanced considerably since some of the earlier development by Noda et al. (1974) and Ebersole and Dalrymple (1979). Both of these earlier models were driven by a wave refraction model but with no current feed back. More recently, Yoo and O'Connor (1986b) developed a wave-induced circulation model based upon what could be classified as a hyperbolic-type wave equation; Yan (1987) and Winer (1988) developed their interaction models based upon parabolic approximation of the wave equation.

Five wave and current coupled models were selected for evaluation. Of the five wave models, four were selected from existing literature and one was developed by the authors. The main differences among the 5 models are their governing wave equations and the as-

[1]Graduate Assistant, Coastal and Oceanographic Engineering Department, Univ. of Florida

[2]Professor, Coastal and Oceanographic Engineering Department, 336 Weil Hall, University of Florida, Gainesville, FL 32611, USA

sociated numerical methods; they include two hyperbolic types, two elliptic types, and one parabolic type. Each can be derived from the mild slope equation given by Kirby(1984), with varying degrees of approximations. The current model is governed by the depth-integrated momentum and continuity equations, much the same as given by Ebersole and Dalrymple (1979).

In this paper, the emphasis is on evaluating wave models and their suitability for wave-current interaction modeling. Thus, the current condition is given as input rather than coupled with the circulation model. The evaluation of fully coupled models has been presented in Lee and Wang (1992).

2 Wave equations

The governing equations of the 5 models are all derivable from the linearized mild slope wave-current interaction equation given by Kirby (1984) as follows:

$$\frac{D^2\hat{\phi}}{Dt^2} + (\nabla \cdot U)\frac{D\hat{\phi}}{Dt} - \nabla \cdot (CCg\nabla\hat{\phi}) + (\sigma^2 - k^2 CCg)\hat{\phi} = 0 \tag{1}$$

where, $\hat{\phi}$ is the surface velocity potential
C is the relative phase velocity (σ/k)
Cg is the relative group velocity $(\partial\sigma/\partial k)$
σ is the intrinsic angular frequency $(\sigma^2 = gk\tanh kh)$
ω is the apparent angular frequency
k is the wave number
h is the water depth
U is the steady current velocity vector (u, v).

The intrinsic frequency and wave number for progressive waves are determined by the Doppler equation

$$\omega = \sigma_d + U \cdot \mathbf{K}$$

where σ_d and $\mathbf{K}$ are, respectively, the intrinsic angular frequency and wave number vector with the inclusion of diffraction effect. Ignoring the mean surface gradient in the above equation yields the conventional Doppler equation (see Eq.(9)). If any reflective wave exists in the current field, the intrinsic frequency and wave number of the reflected wave should be determined by a separate Doppler equation. Therefore, wave reflection effects may be included by superposition.

2.1 Hyperbolic-type model I (HM I) [Ohnaka et al., 1988]

The governing equations are a pair of first-order equations which constitute a hyperbolic system similar to the shallow water wave equations. Ito and Tanimoto (1972) first proposed the approach and Copeland (1985) completed the formulation through the application of the mild slope equation. Ohnaka et al. (1988) extended the formulation to a wave and current coexisting field to obtain:

$$[1 + \frac{\sigma}{\omega}(\frac{Cg}{C} - 1)]\frac{\partial\eta}{\partial t} + \nabla \cdot (U\eta) + \nabla \cdot (\frac{CCg\nabla\hat{\phi}}{g}) = 0 \tag{2}$$

$$\frac{\partial\nabla\hat{\phi}}{\partial t} + \omega g\nabla\frac{\eta}{\sigma} = 0 \tag{3}$$

The unknowns to be solved are the wave surface elevation,η, and the gradient of surface velocity potential, $\nabla\hat{\phi}$. It can be shown that in the presence of strong currents these equations will lead to conditions inconsistent with the conservation equation of wave action given by Brethorton and Garett (1968).

2.2 Hyperbolic-type model II (HM II) [Yoo et al., 1986b]

In this second model the governing equations are based on kinematic and dynamic conservation equations of wave properties averaged over both a wave period and a wave length; they are of the following forms:

$$\frac{\partial \mathbf{K}}{\partial t} + (Cg\frac{\mathbf{K}}{k} + U)\cdot\nabla\mathbf{K} + \mathbf{K}\cdot\nabla U + \frac{k\sigma}{\sinh 2kh}\nabla h - \frac{CCg}{2a}\nabla[\nabla^2(\frac{a}{\sigma})] = 0 \tag{4}$$

$$\frac{\partial}{\partial t}(\frac{a^2}{\sigma}) + \nabla\cdot[(Cg\frac{\mathbf{K}}{k} + U)\frac{a^2}{\sigma}] = 0 \tag{5}$$

Eqs.(4) and (5) are used to solve for $\mathbf{K}$ and a^2/σ.

2.3 Elliptic-type model I (EM I)

The surface velocity potential is now assumed to be a harmonic function of time expressed as:

$$\hat{\phi}(\mathbf{x},t) = \tilde{\phi}(\mathbf{x})e^{-i\omega t}$$

where $\tilde{\phi}(\mathbf{x})$ is the surface potential in steady state. Substituting the above equation into Eq.(1) gives,

$$\begin{aligned} -i\omega\{2U\cdot\nabla\tilde{\phi} + \tilde{\phi}(\nabla\cdot U)\} + (U\cdot\nabla)(U\cdot\nabla\tilde{\phi}) + (\nabla\cdot U)(U\cdot\nabla\tilde{\phi}) \\ -\nabla\cdot(CCg\nabla\tilde{\phi}) + (\sigma^2 - \omega^2 - k^2CCg)\tilde{\phi} = 0 \end{aligned} \tag{6}$$

The above equation together with the Doppler equation permits us to solve for $\tilde{\phi}(\mathbf{x})$.

2.4 Elliptic-type model II (EM II) [Jeong, 1990]

The surface velocity potential is approximated by wave-period and wave-length averaged quantity as,

$$\hat{\phi}(\mathbf{x},t) = A(\mathbf{x})e^{i\psi} = A(\mathbf{x})e^{i(\int \mathbf{K}\cdot d\mathbf{x} - \omega t)} \tag{7}$$

Substituting the above equation into the linearized free surface boundary conditions, we obtain

$$A = -i\frac{g}{\sigma_d}a \tag{8}$$

$$\sigma_d^2 = \sigma^2 - \frac{g}{A}\nabla A\cdot\nabla\bar{\eta} \tag{9}$$

Where σ_d is the intrinsic angular frequency with diffraction effect as mentioned earlier, and $\bar{\eta}$ is the mean surface elevation. The second term in Eq.(9) can be usually be neglected. Substituting Eqs.(7-9) into Eq.(1) and after some manipulation the real and imaginary parts yield two equations; the real part is the energy conservation equation of elliptic type,

$$\nabla\cdot[(Cg\frac{\mathbf{K}}{k} + U)\frac{a^2}{\sigma}] = 0 \tag{10}$$

and the imaginary part is the Eikonal equation,

$$CCg\frac{a}{\sigma}K^2 - \nabla\cdot(CCg\nabla\frac{a}{\sigma}) - k^2CCg\frac{a}{\sigma} = 0 \tag{11}$$

Since there are 3 unknowns, a, K_x and K_y, another equation expressing the irrotationality of wave number is introduced.

$$\nabla \times \mathbf{K} = 0 \tag{12}$$

2.5 Parabolic-type model (PM) [Winer, 1988]

The parabolic approximation to the elliptic-type equation of harmonic wave motion (Eq.6) is derived by 1) splitting the surface potential into two components ($\tilde{\phi} = \tilde{\phi}^+ + \tilde{\phi}^-$) and 2) assuming that the waves are oriented in the x-direction, thus, allowing $k_y \cong 0$. There were several approaches with varying degrees of approximations to arrive at various terms of parabolic equation. The version suggested by Winer (1989) has the final form,

$$\sigma(Cg_x + u)\frac{\partial A'}{\partial x} + i(k_o - k_x)(Cg_x + u)A' + \frac{1}{2}\frac{\partial}{\partial x}[\sigma(Cg_x + u)]A' = \frac{i}{2}\frac{\partial}{\partial y}(CCg\frac{\partial A'}{\partial y}) - \frac{\omega}{2}\frac{\partial v}{\partial y}A' - \omega v\frac{\partial A'}{\partial y} \tag{13}$$

where

$$A' = \tilde{\phi}^+ e^{-ik_o x}, \qquad Cg_x = Cg\frac{k_x}{k}$$

3 Numerical schemes

The numerical methods of all models fall under the category of finite difference method (FDM). Table 1 summarizes the numerical schemes as well as the unknowns of each model. The downwave and side boundary conditions are summarized in Table 2. A brief description of the numerical scheme of each model is given here.

Table 1

Model	Unknowns	Numerical scheme
HM I	η and $\nabla\tilde{\phi}$	FDM on a staggered grid system
HM II	a and $\mathbf{K}$	FDM on a staggered grid system
EM I	complex $\tilde{\phi}$	Combined Gragg's method-FDM
EM II	a, K and θ	Generalized Lax-Friedrich FDM
PM	complex A'	Crank-Nicholson FDM

Table 2

Model	Downwave B.C.	Side B.C.
HM I	Method of chracteristics	$\mathcal{D}_y\eta = ik_y\eta$
HM II	$\mathcal{D}_x a = 0$, $\mathcal{D}_x K_x = 0$	K_y given by Snell's law
EM I	–	$\mathcal{D}_y\tilde{\phi} = ik_y\tilde{\phi}$
EM II	$\mathcal{D}_x a = 0$, $\mathcal{D}_x\theta = 0$	θ given by Snell's law
PM	–	$\mathcal{D}_y A' = ik_y A'$

$\mathcal{D}$=finite difference operator

3.1 Hyperbolic model I

The numerical technique is based on Ohnaka et al. (1988). However, the technique of treating boundary conditions and calculating wave angles has been improved by the introduction of the complex variables as given in Table 2. For details see Lee and Wang (1992).

In the case of wave-current interaction, the determination of wave angle is very important because phase speed, group velocity and intrinsic frequency are determined through the dispersion equation which contains the scalar product of the current vector and the wave number vector. The wave angle is calculated at the center of each grid location by the approximation

$$\theta \cong \tan^{-1}\left[\frac{\mathcal{R}e(\nabla_y \hat{\phi}/\eta)}{\mathcal{R}e(\nabla_x \hat{\phi}/\eta)}\right]$$

and the wave height is calculated by

$$H = 2\sqrt{\mathcal{R}e\{\eta\}^2 + \mathcal{I}m\{\eta\}^2}$$

3.2 Hyperbolic model II

The numerical scheme used here is the same as detailed in Yoo and O'Connor (1986a). The wave amplitude is specified at the center of the grid whereas the wave number vector is situated at the side of the grid.

The wave angle is calculated at the center of each grid location

$$\theta = \tan^{-1}\left(\frac{K_y}{K_x}\right)$$

where the wave number vector indicates the value at the center of each grid and the wave angle is measured from the x-axis.

3.3 Elliptic model I

The numerical scheme was developed by the authors. Here, Eq.(6) is treated as an ordinary differential equation in x while letting the y-direction differential operator, $\mathcal{D}$, be approximated by a finite difference scheme,

$$\begin{aligned}(u^2 - CCg)\tilde{\phi}_{xx} + \{-2i\omega u + 2uu_x + u_y v + uv_y - (CCg)_x\}\tilde{\phi}_x \\ +2uv\mathcal{D}_y(\tilde{\phi}_x) + \{-2i\omega v + 2vv_x + uv_x + u_x v - (CCg)_y\}\mathcal{D}_y(\tilde{\phi}) \\ +(v^2 - CCg)\mathcal{D}_{yy}(\tilde{\phi}) + \{-i\omega(u_x + v_y) + \sigma^2 - \omega^2 - k^2 CCg\}\tilde{\phi} = 0\end{aligned}$$

in which subscripts indicate the differentiations.

The above equation is then converted into a pair of first-order equations by the simple expediency of defining the derivative as a second function.

$$\begin{aligned}\tilde{\phi}_x &= \tilde{\phi}_1 \\ \tilde{\phi}_{1x} &= \frac{1}{u^2 - CCg}[\{-2i\omega u + 2uu_x + u_y v + uv_y - (CCg)_x\}\tilde{\phi}_1 \\ &\quad +2uv\mathcal{D}_y(\tilde{\phi}_1) + \mathcal{F}(\tilde{\phi})]\end{aligned}$$

where

$$\begin{aligned}\mathcal{F}(\tilde{\phi}) &= \{-2i\omega v + 2vv_x + uv_x + u_x v - (CCg)_y\}\mathcal{D}_y\tilde{\phi} + (v^2 - CCg)\mathcal{D}_{yy}\tilde{\phi} \\ &\quad +(-i\omega(u_x + v_y) + \sigma^2 - \omega^2 - k^2 CCg)\tilde{\phi}\end{aligned}$$

These ordinary differential equations are solved numerically using Gragg's method for which the main algorithm for a differential equation $\phi'(x) = f(x, \phi(x))$ is given as

$$\begin{aligned} y_1 &= \phi_{i-1} + hf(x_{i-1}, \phi_{i-1}) \\ y_{j+1} &= y_{j-1} + 2hf(x_{i-1} + jh, y_j) \qquad j = 1, 2, .., n-1 \\ \phi_i &\cong (y_n + y_{n-1} + hf(x_i, y_n))/2 \end{aligned}$$

where h is a subgrid space defined as $h = \Delta x/n$.

The upwave boundary condition is merely the specified complex $\tilde{\phi}$ determined by the incident wave amplitude and wave angle. The side boundary conditions are either non-reflective or reflective. The non-reflective boundary condition can be specified by Snell's law in the absence of diffraction,

$$\tilde{\phi}_y = ik_y\tilde{\phi} \qquad \text{where } k_y = k\sin\theta = k_o\sin\theta_o$$

The reflective boundary condition is expressed as

$$\tilde{\phi}_y = 0 \qquad \text{i.e. } k_y = 0$$

If there is any reflective structure posed in the y-direction, the direction of the reflected waves is the mirror image of that of the incident wave. Since the unknown in this model is the complex surface potential, the reflected wave field can be easily specified as the conjugate by tracing the computation backward.

The wave angle is calculated by

$$\theta = \tan^{-1}\left(\frac{K_y}{K_x}\right)$$

where

$$K_x = \mathcal{I}m\left\{\frac{\tilde{\phi}_1}{\tilde{\phi}}\right\}, \qquad K_y = \mathcal{D}_y^{\pm}S$$

with

$$\begin{aligned} S &= \mathbf{K}\cdot\mathbf{x} = \tan^{-1}[\mathcal{I}m(\tilde{\phi})/\mathcal{R}e(\tilde{\phi})] \\ \mathcal{D}_y^{\pm}S &= [S_{j+1} - S_j]/\Delta y \quad \text{or} \quad [S_j - S_{j-1}]/\Delta y \end{aligned}$$

The wave height is calculated easily by

$$H = 2\sqrt{\mathcal{R}e\{\frac{\sigma}{g}\tilde{\phi}\}^2 + \mathcal{I}m\{\frac{\sigma}{g}\tilde{\phi}\}^2}$$

3.4 Elliptic model II

By introducing wave angle, θ, Eq.(11) can be expressed as,

$$\mathcal{A}K^2 - \mathcal{C} = 0$$

where,

$$\mathcal{A} = CCg\frac{a}{\sigma}, \qquad \mathcal{C} = \nabla\cdot(CCg\nabla\frac{a}{\sigma}) + k^2CCg\frac{a}{\sigma}$$

The solution of K is simply,

$$K = \sqrt{\frac{\mathcal{C}}{\mathcal{A}}}$$

The generalized Lax-Friedrich method is employed to solve Eqs.(10) and (12). Both unknown, θ and a, are solved row by row using an explicit FDM (Ebersole et al. (1986) or Jeong (1990)).

3.5 Parabolic model

Eq.(13) is solved by the Crank-Nicolson scheme using a double sweep approach. The first sweep is required to approximate the x-directional component of group velocity.

The wave angle is calculated by

$$\theta = \tan^{-1}\left(\frac{K_y}{K_x}\right)$$

where

$$K_x \cong k\sqrt{1-(K_y/k)^2}, \qquad K_y = \mathcal{D}_y^{\pm}S$$

with

$$\begin{aligned} S &= \int K_x dx - k_o x + K_y y = \tan^{-1}[\mathcal{I}m(A')/\mathcal{R}e(A')] \\ \mathcal{D}_y^{\pm}S &= [S_{j+1}-S_j]/\Delta y \quad \text{or} \quad [S_j - S_{j-1}]/\Delta y \end{aligned}$$

The wave height is calculated by,

$$H = 2\sqrt{\mathcal{R}e\{\frac{\sigma}{g}A'\}^2 + \mathcal{I}m\{\frac{\sigma}{g}A'\}^2}$$

4 Comparisons of wave models

4.1 Basic equation

The nature and the exactness of the basic equations in each model are evaluated in terms of dynamics (energy conservation) and kinematics (Eikonal equation). The comparisons are summarized in Table 3. For details see Lee and Wang (1992).

Table 3

Model	Assumption	Energy eq.	Eikonal eq.	Violating cond.
HM I	$g\eta \cong i\sigma\hat{\phi}$	approx.	exact	strong current
HM II	$\nabla(CCg) \cong 0$	exact	approx.	steep slope
EM I	–	exact	exact	–
EM II	–	exact	exact	–
PM	$k_y \cong 0$	approx.	approx.	wide angle

4.2 Computational difficulty

The degree of computational difficulty is measured in terms of stability as well as CPU time. The stability criteria given below are obtained for ideal cases only. Therefore, they are not general as well as not vigorous.

Table 4

Model	Stability
HM I	$\Delta t \leq T/[(L_{max}/\Delta x)^2 + (L_{max}/\Delta y)^2]^{1/2}$
HM II	$\Delta t \leq T/[(n_a L_{max}/\Delta x)^2 + (n_a L_{max}/\Delta y)^2]^{1/2}$
EM I	$\Delta y \geq L_{max}/\pi$ for central difference method
EM II	$\Delta y \geq L_{max}/\pi$ for $\tau = 0$
PM	stable

$n_a = Cg_a/C_a$ (with subscript a indicating the absolute)

The comparison for the computational time is also not general. Rather, a specific configuration as shown in Fig.1 is used as the test bench mark. This configuration is a cicular shoal used by Ito and Tanimoto (1972) in their laboratory experiment to study combined diffraction and refraction. This configuration has been cited by many authors for verification purposes. Here, the same grids and same accuracy criteria are used in all models. Wave heights along three cross-sections as shown in Fig.2 are compared with the laboratory data of Ito and Tanimoto. The CPU time on a VAX-8350 computer and the values of the agreement parameter are given below.

Table 5

Model	CPU time	d(Sec.1)	d(Sec.2)	d(Sec.3)
HM I	15 min	0.98	0.97	0.95
HM II	12 min	0.97	0.97	0.96
EM I	24 sec	0.96	0.97	0.94
EM II	5 min	0.98	0.97	0.96
PM	17 sec	0.97	0.97	0.95

The agreement is based on an index, d, given here as an agreement parameter (Willmott, 1981):

$$d = 1 - \frac{\sum_i^N (P_i - O_i)^2}{\sum_i^N (|P_i - \bar{O}| + |O_i - \bar{O}|)^2}$$

where P_i is the numerical value, O_i is the theoretical or observed value and $\bar{O}$ is the mean of the variates O_i. The values for d vary between 0 and 1.0, with 1.0 indicating perfect agreement.

4.3 Wave shoaling and refraction

To test wave shoaling and refraction, numerical results were compared with the analytical solutions based on the energy conservation equation and Snell's law for waves propagating over a uniform slope. The input data are uniformly given to each model as follows:

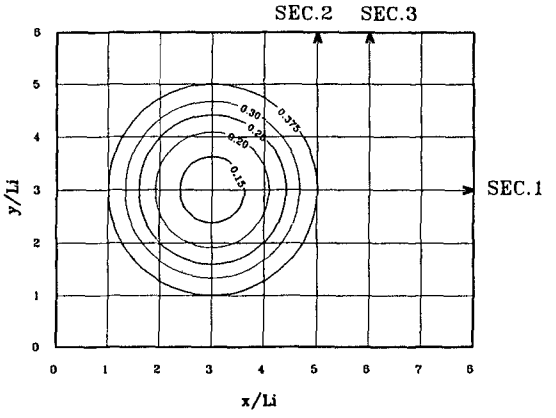

Figure 1: Shoal configuration for comparison of CPU time (concentric circular contours of h/L_i).

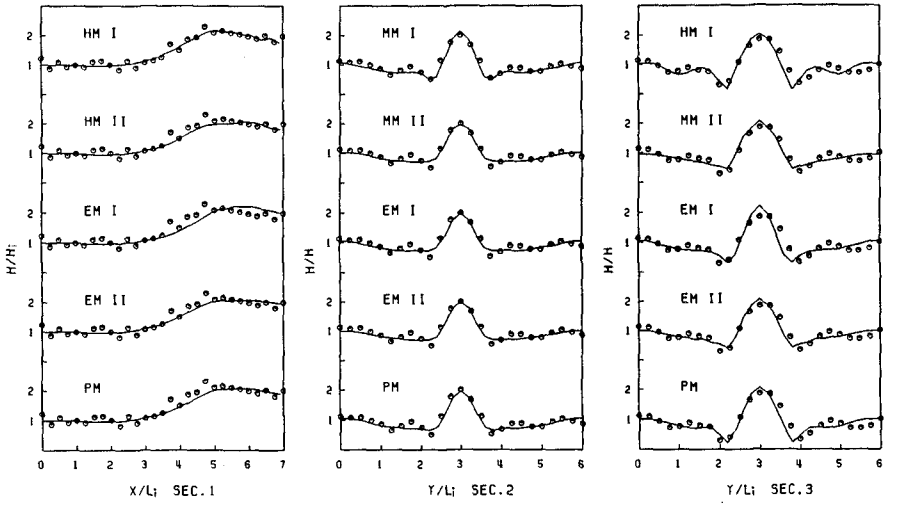

Figure 2: Comparison with the laboratory data of Ito and Tanimoto (1972).

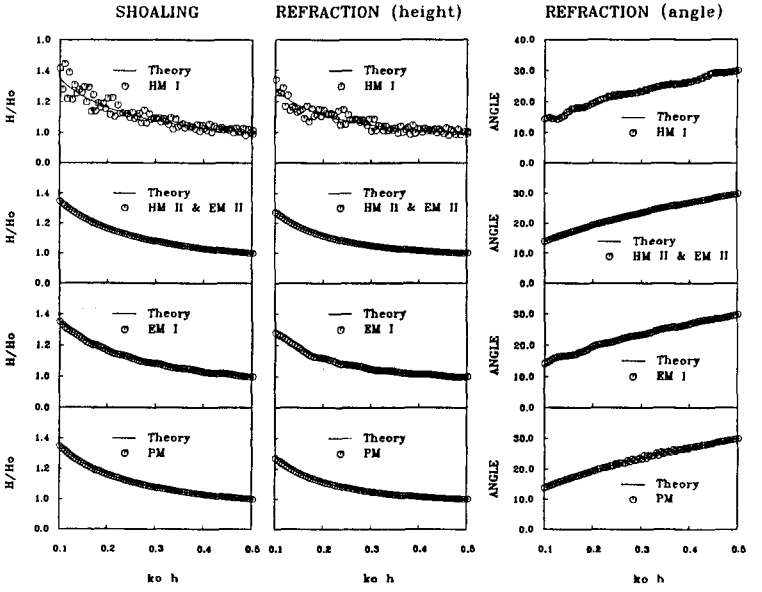

Figure 3: Comparison of wave shoaling and wave refraction.

NX	NY	$\Delta x(m)$	$\Delta y(m)$	$T(sec)$
101	21	0.02	0.14	0.8

The time step in the hyperbolic models is fixed at 0.01 *sec*.

As shown in Figure 3, all models except hyperbolic model I produce results of good agreement. Hyperbolic model I, on the other hand, induces periodical fluctuations. The numerical error appears to be related to the ratio of grid size to wave length. As the wave length shortens towards shoreline the error becomes larger and also propagates up-wave as time progresses. The numerical results were taken along a center grid line in x- axis.

4.4 Wave diffraction

Wave diffraction was evaluated by comparing wave height with the analytical solution given by Wiegel (1962) for a semi-infinite breakwater. The input data are uniformly given as NX=91, NY=75, Δx=0.04 m (=0.1 L), Δy=0.08 m for T=0.511 *sec* except elliptic model II where NY=38 and Δy=0.16 m were used to avoid numerical instability. The time step is 0.01 *sec* in the hyperbolic models.

Figure 4 shows the comparisons for waves approaching normal to the breakwater axis. All models appear to agree well with the analytical result. For 30° angle to the normal, however, only hyperbolic model I and elliptic model II perform adequately (Fig.5). The performance in general can be improved by reducing Δy, except elliptic model II which is almost stable regardless the size of Δy.

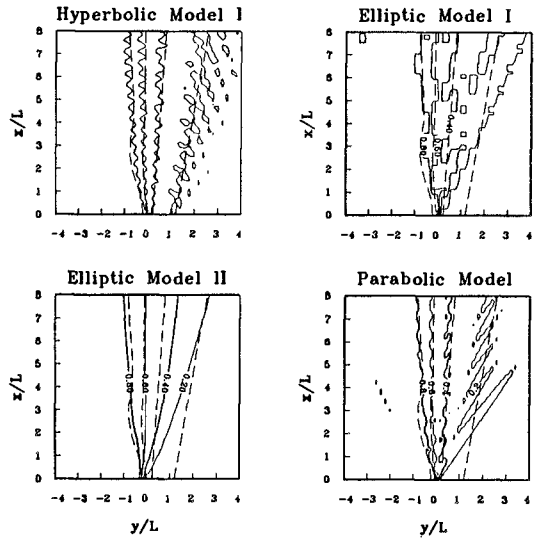

Figure 4: Comparison of wave diffraction for semi-infinite breakwater (0°) between analytic solutions (dotted line) and numerical solutions (solid contour line of 0.8, 0.6, 0.4 and 0.2 diffraction coeff. from left).

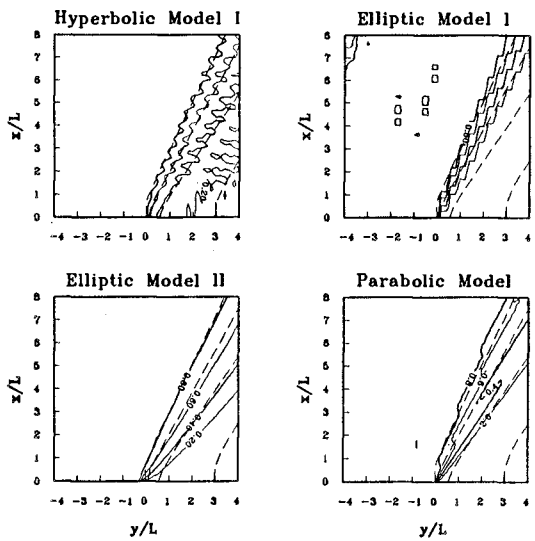

Figure 5: Comparison of wave diffraction for semi-infinite breakwater (30°).

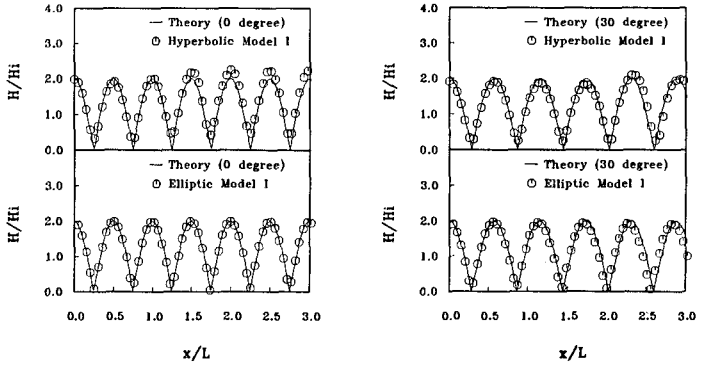

Figure 6: Wave reflection tests against wall.

4.5 Wave reflection

Wave reflection was tested for the case of waves approaching a seawall at 0° and 30° in constant deep water depth of 3 m, using the listed input conditions,

input data	NX	NY	$\Delta x(m)$	$\Delta y(m)$	$\Delta t(sec)$	$T(sec)$
HM	61	21	0.08	0.08	0.02	1.0
EM I	61	21	0.08	0.50	–	1.0

Owing to the finite grid size and time step a numerical error is also expected. Figure 6 shows that the numerical results, on the whole, agree well with theory for both 0° and 30° wave angles. The hyperbolic model tends to yield slightly larger error in wave height, whereas the elliptic model I produces slightly larger phase error.

The wave reflection against the bottom slope was also compared with the 3-dimensional numerical solution represented by Booij (1983). Both models run in this study give reasonablly good agreement as shown in Fig.7.

4.6 Wave-current interaction

Wave-current interaction is compared for cases of colinear current and wave refraction due to the shearing current, both in constant deep water depth of 3 m. The analytic solution for the shearing current is given by Longuet-Higgins and Stewart (1961). The given wave conditions are H_i=0.1 m at the upwave boundary and T=1 sec. Waves are allowed to freely pass through the downwave boundaries. The input data are uniform with NX=101, NY=21, Δx=0.1 m Δy=0.6 m for the elliptic models and Δy=0.1 m for the rest. Δt, whenever applicable, is taken as 0.01 sec.

The comparisons with analytical solutions are given in Fig.8. For the colinear case, all except hyperbolic model I performed adequately. For non-colinear case, hyperbolic model II and elliptic model II yield good results; the rest all produce varying degrees of inconsistency.

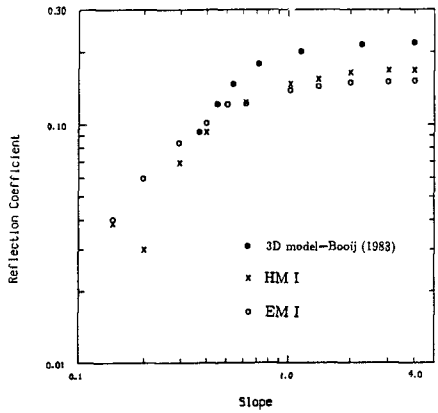

Figure 7: Wave reflection tests against bottom slope.

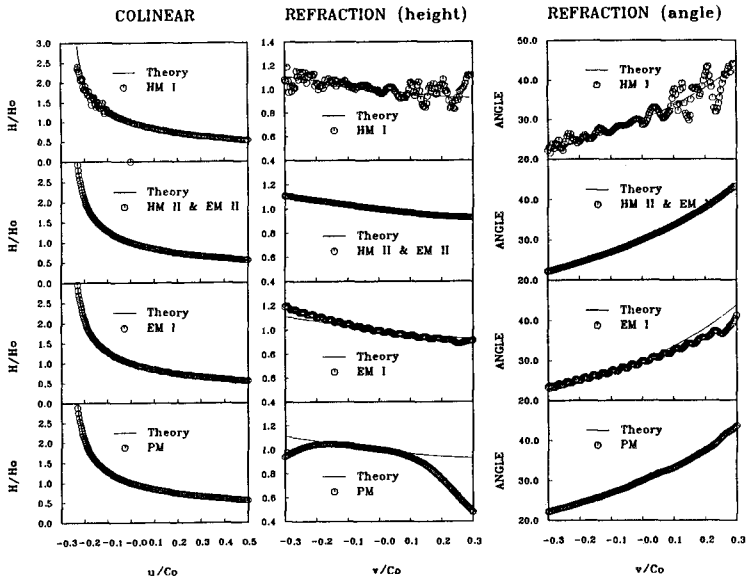

Figure 8: Wave-current interaction comparison.

4.7 Summary

Each model was evaluated or run on a number of bench mark cases. The final evaluations with assigned rankings are given in the following matrix:

Table 6

Case	HM I	HM II	EM I	EM II	PM
Governing equation	M	O	O	O	M
Programming ease	O	M	O	M	O
Numerical stability	M	X	X	X	O
Computational time	X	X	O	M	O
Shoaling	O	O	O	O	O
Refraction	M	O	M	O	M
Diffraction (normal)	O	O	O	O	O
Diffraction (oblique)	O	O	X	O	M
Reflection (vertical)	O	–	O	–	–
Reflection (slope)	O	–	O	–	–
Current (colinear)	M	O	O	O	O
Current (refraction)	X	O	M	O	X

O: good M: marginal X: bad –: not applicable

5 Conclusions

Five numerical wave-current interaction models were evaluated in a two-dimensional domain through mutual comparisons. The evaluation is limited in that the bench mark cases are restricted to those with either theoretical solution or accepted hydraulic model results. Within this context, the performance of each model is evaluated, and the comparisons are given in a matrix form. At this moment, there appears to be no single model that clearly outperforms the others. The selection of a model for application depends upon the intended purpose. Therefore, the present paper should serve as a useful guilde line for model selection.

References

[1] Berkhoff, J.C.W., 1972. "Computation of combined refraction-diffraction," Proc. 13th ICCE, ASCE, pp.471-490.

[2] Booij, N., 1983. "A note on the accuracy of the mild slope equation," Coastal Eng., Amsterdam Netherlands, Vol. 7, pp.191-203.

[3] Brethorton, F.P. and C.J.R. Garrett, 1969. "Wave trains on inhomogeneous moving media," Proc. Royal Society of London, London, England, Series A, Vol. 302, pp.529-554.

[4] Copeland, G.J.M., 1985. "A practical alternative to the mild slope wave equation," Coastal Eng., Amsterdam Netherlands, Vol. 9, pp.125-149.

[5] Dalrymple, R.A., K.D. Suh, J.T. Kirby and J.W. Chae, 1989. "Models for very wide-angle water waves and wave diffraction. Part 2. Irregular bathymetry," J. Fluid Mech. Vol. 201, pp.299-322.

[6] Ebersole, B.A. and Dalrymple R.A., 1979. "A numerical model for nearshore circulation including convective accelerations and lateral mixing," Ocean Engineering Report No. 21, Dept. of Civil Eng., Univ. of Delaware, Newark, Delaware.

[7] Ebersole, B.A., M.A. Cialone and M.D. Prater, 1986. "Regional coastal processes numerical modeling system," Report 1, RCPWAVE-A linear wave propagation model for engineering use, Technical report CERC-86-4, US Army Engineer WES, Vicksburg, Mississippi.

[8] Ito, Y. and K. Tanimoto, 1972. "A method of numerical analysis of wave propagation-Application to wave diffraction and refraction," Proc. 13th ICCE, ASCE, pp.503-522.

[9] Jeong, S.T., 1990. "Wave transformation in regions of slowly varying depths with currents", Ph.D dissertation, Dept. of Civil Engineering, Seoul National Univ., Seoul, Korea.

[10] Kirby, J.T., 1984. "A note on linear surface wave-current interaction over slowly varying topography," J. Geophysical Research, Vol. 89, No. C1, pp.745-747.

[11] Lee, J.L. and H. Wang, 1992. "Evaluation of wave models coupled with the circulation model," UFL/COEL-92/014, Coastal and Oceanographic Engineering Department, Univ. of Florida, Gainesville.

[12] Longuet-Higgins, M.S. and R.W. Stewart, 1961. "The changes in amplitude of short gravity waves on steady non-uniform currents, J. Fluid Mech., Vol. 10, pp.529-549.

[13] Noda, E., C.J. Sonu, V.C. Rupert and J.I. Collins, 1974. "Nearshore circulation under sea breeze conditions and wave-current interactions in the surf zone," Tetra Tech Report TC-149-4.

[14] Ohnaka, S., A. Watanabe and M. Isobe, 1988. "Numerical modeling of wave deformation with a current," Proc. 21th ICCE, ASCE, pp.393-407.

[15] Radder A.C., 1979. "On the parabolic equation for water-wave propagation," J. Fluid Mech., Vol. 95, pp.159-176.

[16] Wiegel, R.L., 1962. "Diffraction of waves by a semi-infinite breakwater," J. Hydraulics Div., ASCE, Vol. 88, No. HY1, pp.27-44.

[17] Willmott, C.J., 1981. "On the validation of models," Phys. Geog. Vol. 2, pp.184-194.

[18] Winer, H.S., 1988. "Numerical modeling of wave-induced currents using a parabolic wave equation," Ph.D dissertation, Coastal and Oceanographic Engineering Department, Univ. of Florida, Gainesville.

[19] Yan, Y., 1987. "Numerical modeling of current and wave interaction on an inlet-beach system," Technical Report No. 73, Coastal and Oceanographic Engineering Department, Univ. of Florida, Gainesville.

[20] Yoo, D. and B.A. O'Connor, 1986a. "Mathematical modeling of wave-induced nearshore circulations," Proc. 20th ICCE, ASCE, pp.1667-1681.

[21] Yoo, D. and B.A. O'Connor, 1986b. "Ray model for caustic gravity waves," Proc. 5th Congress of Asian and Pacific Division, IAHR, Vol. 3, pp.1-13.